Effect of Platelet Rich Plasma Versus Spontaneous Healing in Induced Muscle Injury in Senile Male (Albino Rats)

Original Article

Yara Hassan Mohamed[1], Shahira Youssef Mikhail[2], Rehab Tolba Khattab, Noha Mohamed Gaber[2], Hala Taha Shalan[2] and Mary Refaat Isaac[2]

Department of Anatomy and Embryology, Faculty of Medicine, [1]Suez university,

[2]Ain Shams University, Egyp

ABSTRACT

Introduction: Falls, with subsequent fracture and muscle injury are very commonly encountered in the elderly. Platelet rich plasma has been found to have marked ability to enhance regeneration of various tissues and organs and is widely used nowadays in a variety of medical sectors.

Aim of the Work: To study the effect of PRP on skeletal muscle repair in senile male albino rats.

Material and Methods: Forty-two senile male senile albino rats, aging 24 months and weighing 280 grams, were used. Six rats were used as PRP donors and thirty-six were equally divided into three groups. Group I was equally subdivided into subgroup IA; rats were left without intervention and subgroup IB; rats were sham operated on the right hind limb. Group II: gastrocnemius muscle injury was induced in the right hind limb and rats were left for spontaneous healing and were further equally subdivided into subgroups IIA and IIB where rats were sacrificed on the 1st day and the 7th day post-injury respectively. Group III: gastrocnemius muscle injury was induced as group II, and rats were treated with 100 microliters PRP on the same day of injury then rats were further equally subdivided into subgroup IIIA: rats were sacrificed on the 1st day post-injury and subgroup IIIB: rats were given 100 microliters of PRP on the 3rd day and 5th day post- injury then were sacrificed on the 7th day. At the end of experiment for each subgroup, the gastrocnemius muscle was excised and processed for light and transmission electron microscopic examination.

Results: PRP led to stronger post injury acute inflammatory response and prevented the persistence of age-related delayed inflammatory state. Moreover, it markedly enhanced myogenesis and decreased fibrous tissue scaring.

Conclusion: PRP treatment accelerated the rate and improved the quality of skeletal muscle healing in senile rats.

Received: 03 October 2022, **Accepted:** 31 October 2022

Key Words: Aging, inflammatory cells, muscle injury; platelet rich plasma, satellite cells.

Corresponding Author: Yara Hassan Mohamed, PhD, Department of Anatomy and Embryology, Faculty of Medicine, Suez university, Egypt, **Tel.**: +20 10 6000 5423, **E-mail:** yara.hassan@med.suezuni.edu.eg

ISSN: 1110-0559, Vol. 47, No. 1

INTRODUCTION

Musculoskeletal injuries are one of the most common causes of severe, chronic pain and physical disability affecting people all around the world[1]. Skeletal muscle function deteriorates with age, resulting in a steady loss of muscle mass, quality, and strength. One of the major reasons of skeletal muscle dysfunction in the elderly is the lack of regenerative ability[2]. It has been recorded that even if the degree of injury is identical, elderly are found more likely to show greater loss and slower recovery rate in comparison to younger adult[3]. Skeletal muscle healing occurs through a series of overlapping stages including degeneration, inflammation, and regeneration. Aging is associated with increased early deposition of collagenous tissue in skeletal muscle[2] leading to excessive fibrosis which is thought to inhibit regeneration[4]. Platelet-rich plasma (PRP) is one of the most promising therapeutic agents owing to its ability to enhance regeneration of various tissues and organ. Moreover, platelet growth factors (PGFs) were found to support the various stages of the wound healing and repair[5]. Thus, it became the aim of the present study to examine the effect of PRP on skeletal muscle repair in senile rats.

MATERIAL AND METHODS

Animals

Forty-two senile male albino rats, aging 24 months and weighing an average of 280 grams were used in this study. Animals were obtained and locally bred at the animal facility of Faculty of Medicine Ain Shams Research Institute (MASRI). Rats were housed in medium sized metal cages in room temperature, with adequate ventilation, regular dark/light cycles and were given free diet and water access. All rats were kept under the same circumstances throughout the experiment and were given two-weeks acclimatization period prior to the experiment. The experimental protocol was approved by the Committee of Animal Research Ethics (CARE), Faculty of Medicine - Ain Shams University.

 DOI: 10.21608/ejh.2022.166668.1783

Platelet-rich plasma preparation

Six rats were assigned to be PRP donors and were anaesthetized using intra-peritoneal injection of 60 mg/kg pentobarbital before whole blood was extracted from the retro-orbital plexus of vessels using a capillary tube[6]. Blood was immediately deposited in a sodium citrate test tube and centrifuged at 200 g for 15 minutes, separating the sample into three parts: the red bottom fraction, the intermediate yellow-straw fraction (buffy coat), and the top fraction. The top fraction, including the buffy coat, was pipetted, and the pipetted contents were centrifuged at 500 g for 10 minutes. After centrifugation, the bottom PRP content was pipetted and was used in treatment for injured muscles in the assigned groups[7,8].

Muscle injury procedure

After the rats were sedated with an intra-peritoneal injection of 60 mg/kg pentobarbital, the skin of the right hind limb was sterilized then dissected. A number 11 surgical blade was used to make a small incision perpendicular to the muscle fibers in the mid belly of the gastrocnemius muscle. The incision was 5 mm deep and 5 mm long. A suture was put at both ends of the muscle incision to help identify the injury site in the future. Under sterile conditions, the skin incision was restitched[9].

Experimental protocol

Thirty-six rats were equally divided into 3 groups, 12 rats in each, as follows:

Group I (Control): was further equally subdivided into two subgroups:

- Subgroup IA: rats were left without intervention.
- Subgroup IB: rats were sham operated where a 5 mm long incision was done in the skin of the right hind limb in each rat.

Three rats of both subgroups were sacrificed on the 1st day post- injury and three were sacrificed on the 7th day post- injury.

Group II (Untreated muscle injury): muscle injury was induced in the right hind limb in each rat. Then rats were further equally subdivided into two subgroups:

- Subgroup IIA: rats were sacrificed on the 1st day after induction of injury[10].
- Subgroup IIB: rats were sacrificed on the 7th day after induction of injury[11].

Group III (Muscle injury treated with PRP): muscle injury was induced in the right hind limb as group II and rats were treated with 100 microliters PRP on the same day of injury (day 0). Then they were further equally subdivided into two subgroups.

- Subgroup IIIA: rats were sacrificed on the 1st day after induction of injury.
- Subgroup IIIB: rats were given 100 microliters of PRP on the 3rd day and the 5th day and were sacrificed on the 7th day after induction of injury[11].

At the end of experiment for each subgroup, rats were anesthetized using intra-peritoneal pentobarbital prior to sacrifice. Gastrocnemius muscle of the right hindlimb was excised in each group at the site of injury, then processed for light and transmission electron microscopic examination.

Light microscopic examination

Muscle samples were fixed in 10% formalin for 48h, dehydrated, cleared, and embedded in paraffin to create paraffin blocks. Then 5 um sections were cut and stained by Hematoxylin & Eosin stain[12] and Masson's Trichome stain[13]. Olympus light microscope (CX31) in the Anatomy department, Faculty of Medicine, Ain Shams University was used to examine and photograph the stained sections.

Transmission electron microscopic examination

Muscle samples measuring 1 mm^3 were fixed in 2.5% glutaraldehyde for 24 hours, washed twice in phosphate buffer, fixed in 1% osmic acid for one hour at room temperature, washed again twice in phosphate buffer for half an hour each, dehydrated in ascending grades of ethyl alcohol, cleared in propylene oxide for 20 minutes, and embedded in Epon resin. Semithin sections 1 mm in thickness were cut with glass knives on ultramicrotome, stained with 1% toluidine blue with pH 7.3 and examined by an Olympus light microscope to choose the selected areas. Ultrathin sections 50 nm were cut using a glass knife, mounted on copper grids, stained with uranyl acetate for 20 minutes and lead citrate for 10 minutes, and then they were washed in distilled water & preserved in labeled capsules[13]. Electron microscope in the Faculty of Science, Ain Shams University, Egypt, was used to view and photograph the sections.

Morphometric study and statistical analysis

The number of inflammatory cells and the number of regenerating myofibers were counted by (X40) objective lens at the site of injury from H&E-stained sections, using the image J software (V 1.48). In addition, the area percentage of collagen fibers' deposition per microscopic field was measured by (X20) objective lens at the site of injury from Masson's trichrome stained sections, using the image analyzer Leica Q500 MC program in the Histology and Cell Biology Department, Faculty of Medicine, Ain Shams University. The measurements were taken in five randomly chosen non-overlapping fields in each of five stained sections obtained from five animals in each subgroup. The mean and standard deviation of the results were determined. The SPSS application was used to calculate the P value where $P<0.05$ was considered to be significant, $P< 0.001$ highly significant and $P >0.05$ non-significant.

RESULTS

Histological results

Examination of muscle sections of subgroups IA and IB revealed almost similar findings. Hematoxylin and Eosin- stained sections revealed straight, parallel, regular acidophilic myofibers. They demonstrated clear striations and flattened peripheral basophilic nuclei with clear sarcolemma. Delicate connective tissue endomysium in between myofibers was also observed (Figure 1). Masson's trichrome stained sections revealed some collagen fibers in between parallel striated muscle fibers (Figure 2). Semithin sections showed parallel myofibers with prominent striations having peripherally situated flattened nuclei and clear sarcolemma (Figure 3). Ultrathin sections revealed regular sarcomeres extending between two successive Z lines, and the nuclei were seen just under the sarcolemma (Figure 4). Each sarcomere was composed of alternating dark bands (A band) and light bands (I band) (Figure 5). Satellite cell (SC) having oval nuclei with peripheral chromatin condensation as well as some collagen fibers were also observed in between myofibers (Figure 5).

Regarding group II rats where muscle injury was induced and left untreated, examination of H&E-stained section of subgroup IIA rats, which were sacrificed on the 1st day after injury, revealed widely separated, fragmented myofibers accompanied with edema in perimysium. Focal areas of hemorrhage and mononuclear cellular infiltration were also seen (Figure 6). Masson's trichrome stained sections revealed distorted fragmented muscle fibers admixed with large areas of irregular collagen fibers deposition (Figure 7). Semithin sections showed inflammatory cellular infiltration including some neutrophils and macrophages in the damaged area (Figure 8). Ultrathin sections revealed damaged myofibers with disorganized myofibrils, sarcoplasmic loss, and detached sarcolemma (Figure 9) with adjacent areas with almost complete loss of striations (Figures 9,10). Macrophages (Figures 9,10) and numerous neutrophils with multilobed nuclei and clear vesicles together with clumped bundles of collagen fibers were frequently seen in the damaged areas (Figure 11).

Examination of H&E-stained sections of subgroup IIB, where rats were also left untreated but were sacrificed on the 7th day after injury, showed persistent inflammatory cellular infiltration invading and surrounding the damaged muscle fibers (Figure 12). Some regenerating myofibers were also seen (Figure 12). Masson's trichrome stained sections showed marked deposition of densely packed, greenish-colored collagen bundles in the damaged site with some intervening regenerating myofibers (Figure13). Semithin sections showed numerous inflammatory cells including lymphocytes and macrophages among some myoblasts and regenerating myofibers with oval vesicular nuclei (Figure 14). Ultrathin sections revealed some areas with regenerating myotubes containing myoblast cells (Figures 15,16) besides focal areas of hemorrhage (Figure 15) and spindle shaped fibroblast with oval nuclei (Figure 16). However, numerous inflammatory cells including; neutrophils with multilobed nuclei (Figures15,16) and macrophages with large nuclei and abundant cytoplasm (Figures 16,17) were frequently seen with some necrotic debris (Figure 17). Moreover, other areas revealed condensed collagen bundles widely separating myofibers with irregularly organized sarcomeres and sarcoplasmic vacuolations (Figure 18).

Regarding group III rats where muscle injury was induced and treated with PRP, examination of H&E-stained sections of subgroup IIIA rats which were sacrificed on the 1st day after injury revealed edema in perimysium and endomysium in between damaged myofibers. Areas of damaged muscles showed numerous blood vessels among inflammatory cell infiltrate (Figure 19). Masson's trichrome stained sections showed green colored irregular collagen fibers deposition and numerous blood vessels along with nerve trunk at the injury site (Figure 20). Semithin sections showed numerous areas of inflammatory cell infiltrate in between myofibers including several neutrophils and macrophages in addition to necrotic debris (Figure 21). Ultrathin sections showed damaged myofibers with complete loss of muscle striation alongside with nearby muscle fibers with almost normal architecture (Figure 22). Mononuclear myoblast cell, spindle shaped fibroblast with flattened oval nuclei (Figures 22,23), blood vessel (Figure 23) and neutrophils with multilobed nuclei (Figures 23,24) were frequently detected between damaged myofibers. Many of the encountered neutrophils had membrane bound extensions as pseudopodia around necrotic debris, while others had vesicles. Macrophages and scattered bundles of collagen fibers were also detected in the damaged site (Figure 24).

Examination of H&E-stained sections of subgroup IIIB where rats were treated with PRP and sacrificed on the 7th after injury revealed numerous regenerated muscle fibers and some of which were separated by inflammatory cell infiltrate enclosing newly formed blood vessels (Figure25). Masson's trichrome stained sections showed some tightly packed collagen fibers among numerous newly formed myofibers and numerous blood vessels (Figure26). Semithin sections showed numerous newly formed myofilaments and dispersed mononuclear myoblast cells besides large, nucleated macrophages (Figure 27). Ultrathin sections revealed well-formed multinucleated myotube with numerous mitochondria and myofilaments that showed Z lines. Macrophages were also seen in contact with these newly formed myotubes (Figure 28). Moreover, nearby areas showed almost organized sarcomeres with peripheral nucleus and intact sarcolemma. Few amounts of collagen fibers were seen among the myofibers (Figure29).

Statistical Results

Statistical analysis of the morphometric results of the subgroups that were sacrificed on the first day after injury, revealed highly significant increase ($P < 0.001$) in the number of inflammatory cells in the PRP treated

rats (subgroup IIIA) when compared to the untreated ones (subgroup IIA) (Table1, Histogram 1). On the other hand, rats that were sacrificed on the 7th day after muscle injury showed highly significant decrease (P<0.001) in the number of inflammatory cells in the PRP treated rats (subgroup IIIB) when compared to the untreated ones (subgroup IIB) (Table1, Histogram 1).

Statistical analysis of the morphometric results of subgroups that were sacrificed on the 7th day after muscle injury showed highly significant increase (P<0.001) in the number of regenerating myofibers in the PRP treated rats (Subgroup IIIB) when compared to the untreated ones (subgroup IIB) (Table2, Histogram 2).

Statistical analysis of the morphometric results of the subgroups that were sacrificed on the first day after injury, revealed non-significant changes (P > 0.05) in the mean area percentage of collagen fiber deposition between the treated rats (Subgroup IIA) and the untreated ones (Subgroup IIIA). On the other hand, rats that were sacrificed on the 7th day after muscle injury showed significant decrease (P<0.05) in the mean area percentage of collagen fibers deposition in the treated rats (Subgroup IIIB) when compared to the untreated ones (subgroup IIB) (Table3, Histogram 3).

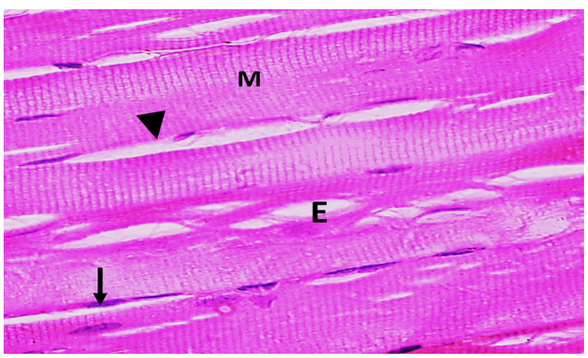

Fig. 1: A photomicrograph of longitudinal section of rat's gastrocnemius of group IA showing peripherally situated flattened nuclei (arrow) within straight parallel acidophilic muscle fibers with apparent striations (M) and clear sarcolemma (arrowhead). Notice the connective tissue endomysium (E) in between muscle fibers containing delicate collagen fibers. H&E (X400)

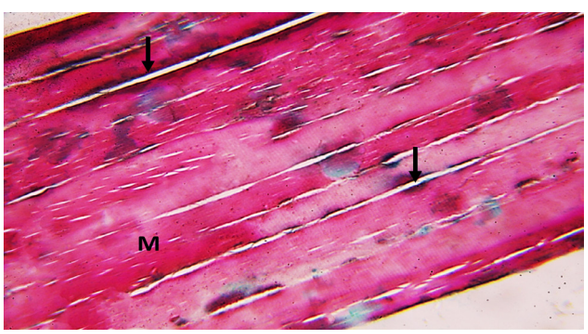

Fig. 2: A photomicrograph of longitudinal section of rat's gastrocnemius of group IA showing few collagen fibers (arrow) in between parallel striated muscle fibers (M). Masson's trichrome (X100)

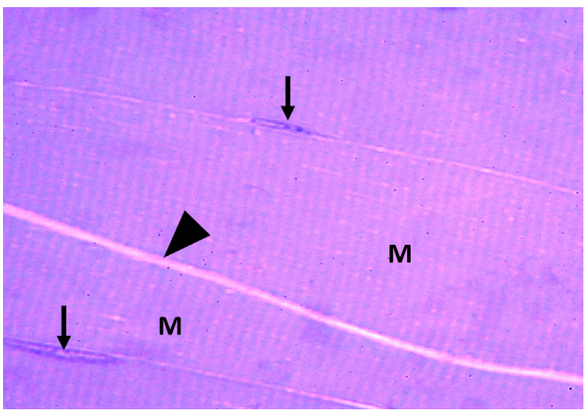

Fig. 3: A photomicrograph of longitudinal section of rat's gastrocnemius of group IA showing prominent cross striations of parallel myofibers (M) having peripherally situated flattened nuclei (arrow) and clear sarcolemma (arrowhead). Toluidine blue (X1000)

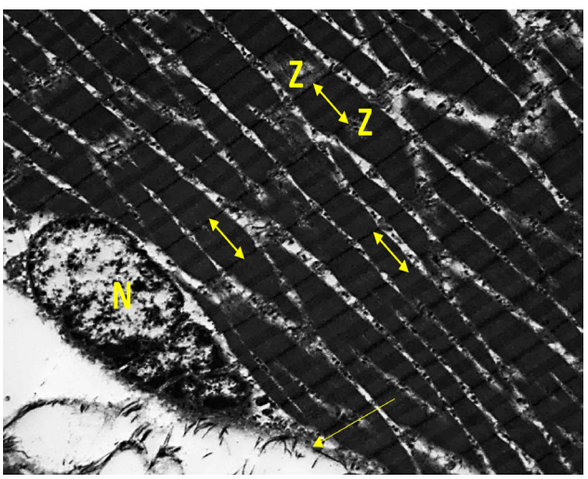

Fig. 4: A photomicrograph of longitudinal section of rat's gastrocnemius of group IA showing regular sarcomeres (↔) extending between two successive Z lines (Z). Nucleus (N) can be seen under the sarcolemma (arrow). TEM (X2000)

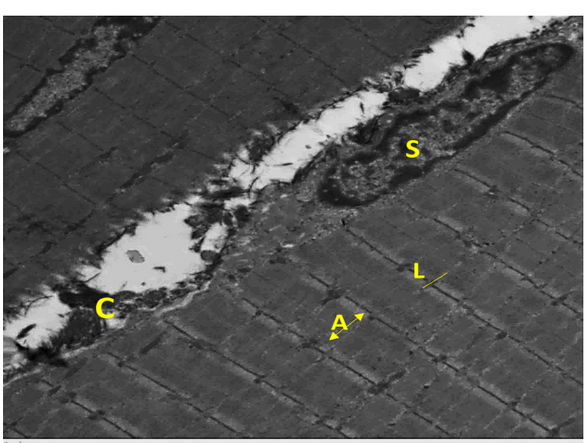

Fig. 5: A photomicrograph of longitudinal section of rat's gastrocnemius of group IA showing adjacent myofibers with normal pattern of the myofibrils with alternating light (L -) and dark (A↔) bands. Notice satellite cell with its peripheral condensed chromatin (S). Note also few collagen fibers (C) in between myofibers. TEM (X2000)

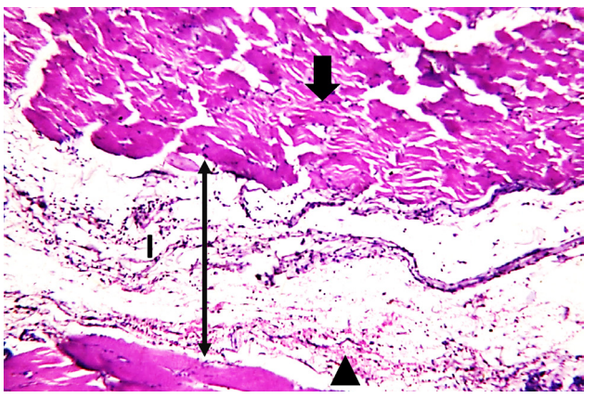

Fig. 6: A photomicrograph of longitudinal section of rat's gastrocnemius of subgroup IIA showing widely separated (↔) fragmented myofibers (arrow) accompanied with focal area of hemorrhage (arrowhead), and inflammatory cell infiltrate (I). H&E (X100)

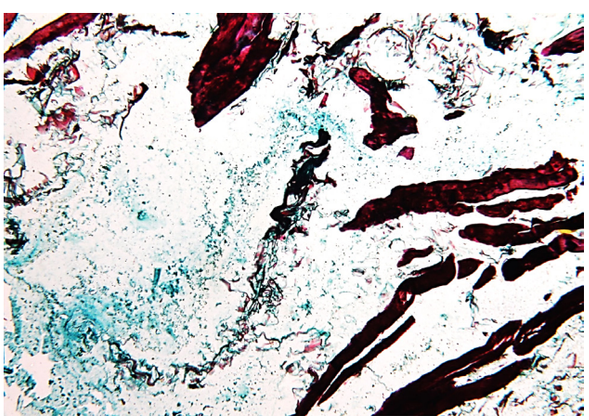

Fig. 7: A photomicrograph of longitudinal section of rat's gastrocnemius of subgroup IIA showing distorted, fragmented red colored muscle fibers admixed with large areas of irregular, greenish colored bundles of collagen fibers deposition. Masson's trichrome (X100)

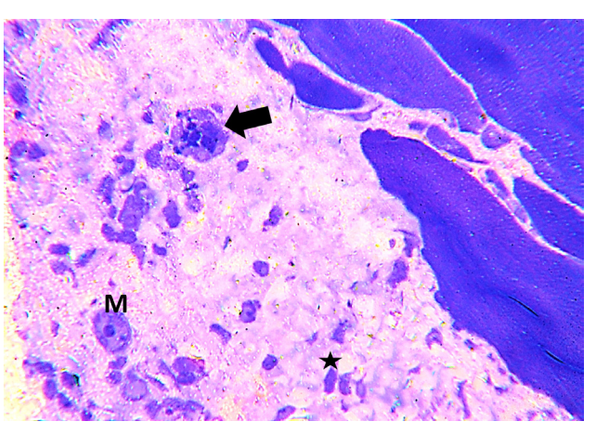

Fig. 8: A photomicrograph of longitudinal section of rat's gastrocnemius of subgroup IIA showing inflammatory cell infiltrate (star). Notice the neutrophil (arrow) and macrophage (M). Toluidine blue (X1000)

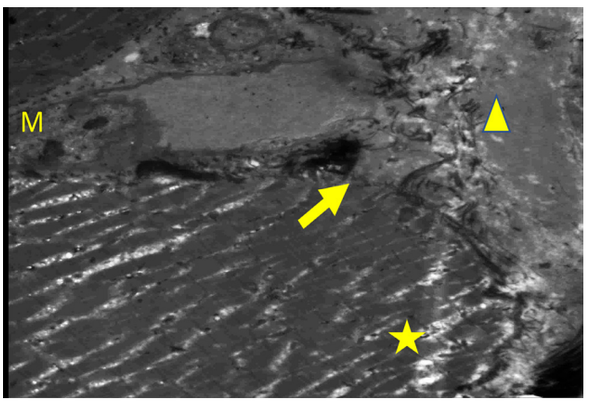

Fig. 9: A photomicrograph of longitudinal section of rat's gastrocnemius of subgroup IIA showing loss of sarcoplasm (star), within disorganized myofibrils, as well detached sarcolemma (arrow). Notice the area with almost complete loss of striations (arrowhead). Note also the macrophage (M). TEM (X1000)

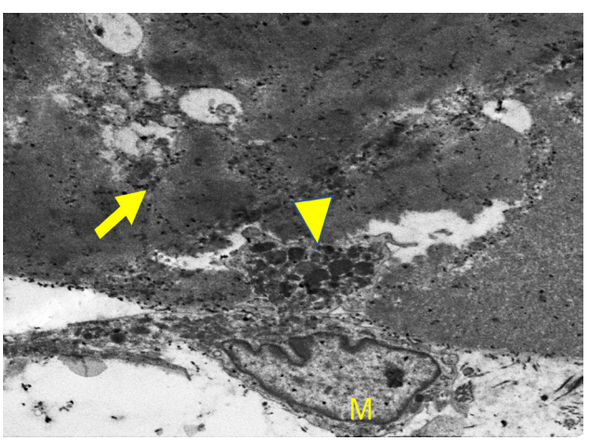

Fig. 10: A photomicrograph of longitudinal section of rat's gastrocnemius of subgroup IIA showing necrotic myofiber with complete loss of muscle striation (arrow). Notice phagocytic cell (arrowhead) and macrophage (M). TEM (X5000)

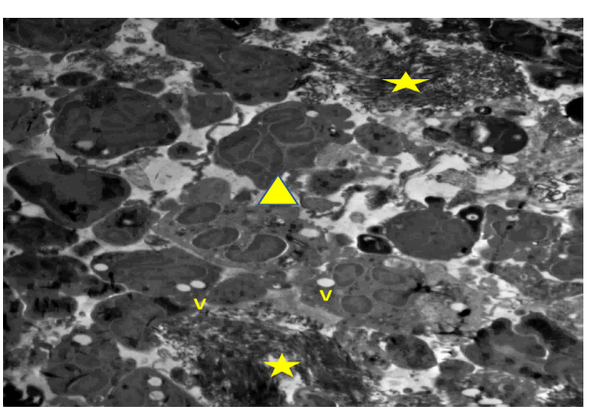

Fig. 11: A photomicrograph of longitudinal section of rat's gastrocnemius of subgroup IIA showing clumped bundles of collagen fibers deposition (star), numerous neutrophils with multilobed nuclei (arrowhead) and clear vesicles (V). TEM (X1000)

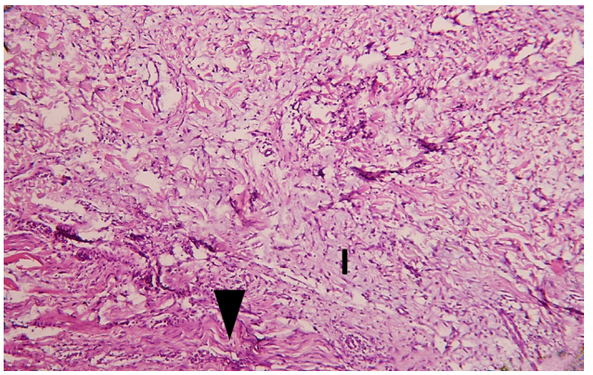

Fig. 12: A photomicrograph of longitudinal section of rat's gastrocnemius of subgroup IIB showing inflammatory cell infiltrate (I) and some regenerating myofibers (arrowhead). H&E (X100)

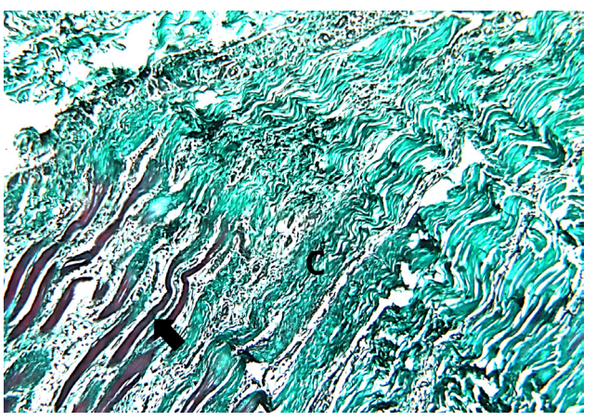

Fig. 13: A photomicrograph of longitudinal section of rat's gastrocnemius of subgroup IIB showing few regenerating myofibers (arrow) within green densely packed collagen fibers bundles in the site of injury (C). Masson's trichrome (X100)

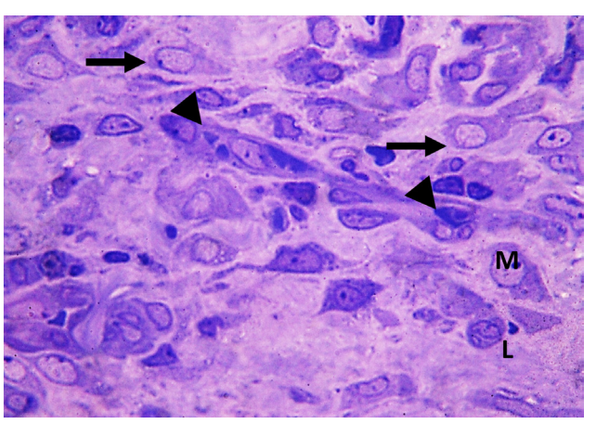

Fig. 14: A photomicrograph of longitudinal section of rat's gastrocnemius of subgroup IIB showing inflammatory cellular infiltration including macrophage (M) and lymphocyte (L). Notice scattered myoblast cells (arrow). Note also regenerating myofiber (arrowhead) with a row of internal vesicular nuclei. Toluidine blue (X1000)

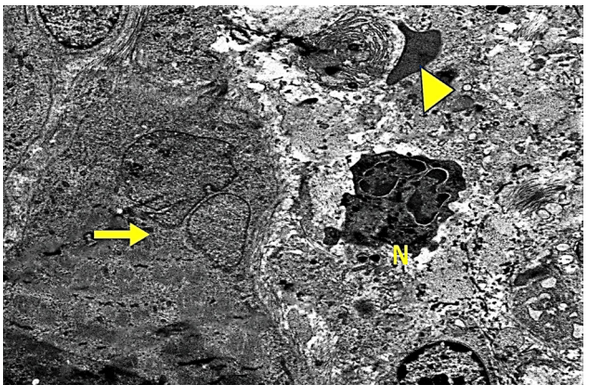

Fig. 15: A photomicrograph of longitudinal section of rat's gastrocnemius of subgroup IIB showing regenerated myofiber with myoblast cell (arrow). Notice multilobed neutrophil nuclei (N) and focal area of hemorrhage (arrowhead). TEM (X5000)

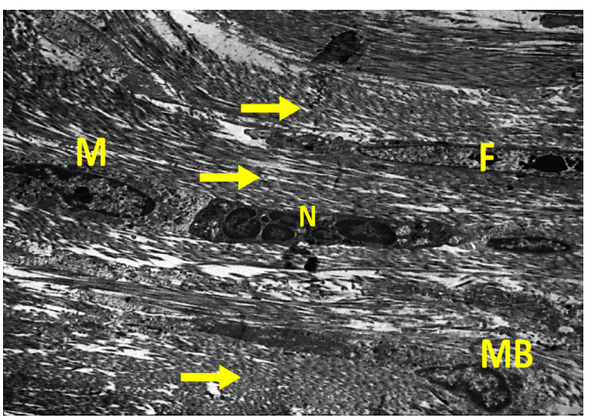

Fig. 16: A photomicrograph of longitudinal section of rat's gastrocnemius of subgroup IIB showing myoblast cell (MB), and immature myofibers without distinct striations (arrows) with aggregations of mononuclear cells as macrophage (M) and fibroblast (F) besides multilobed neutrophil nuclei (N). TEM (X1000)

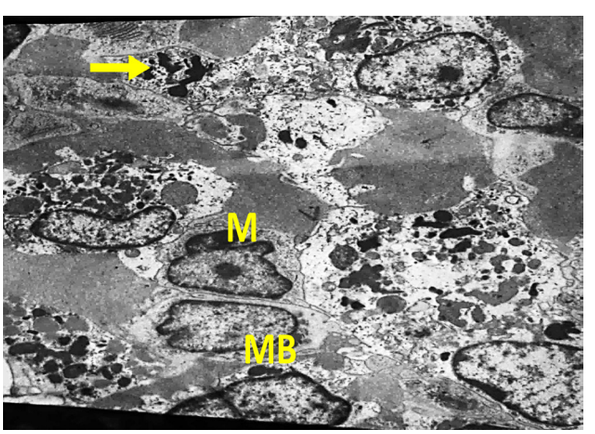

Fig. 17: A photomicrograph of longitudinal section of rat's gastrocnemius of subgroup IIB showing numerous enlarged macrophage (M) and necrotic debris (arrows). Notice myoblast cells (MB). TEM (X1200)

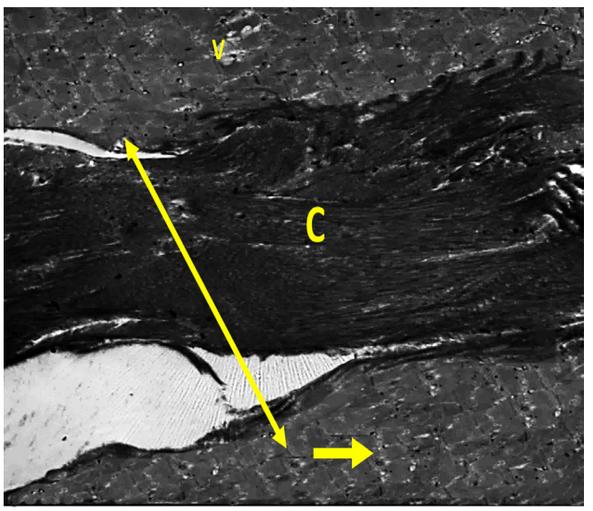

Fig. 18: A photomicrograph of longitudinal section of rat's gastrocnemius of subgroup IIB showing condensed collagen fibers deposition (C), widely separating myofibers (↔) with disorganized sarcomeres (arrow) and sarcoplasmic vacuolations (V). TEM (X1000)

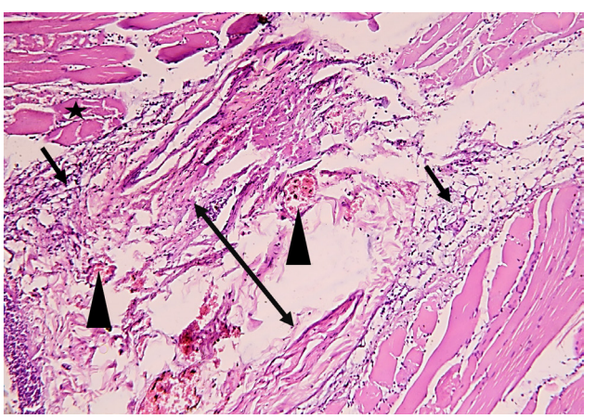

Fig. 19: A photomicrograph of longitudinal section of rat's gastrocnemius of subgroup IIIA showing inflammatory cell infiltrate (arrow), and blood vessels (arrowhead) in between widely separated (↔), damaged muscle fibers (star). H&E (X100)

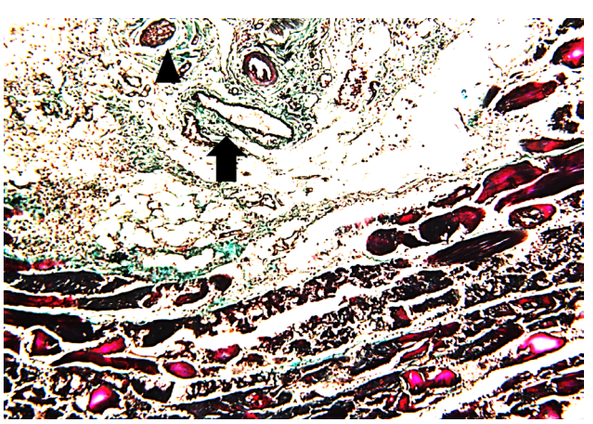

Fig. 20: A photomicrograph of longitudinal section of rat's gastrocnemius of subgroup IIIA showing greenish colored irregular collagen fibers deposition and red stained myofibers. Notice nerve trunk (arrowhead) and numerous blood vessels (arrow). Masson's trichrome (X100)

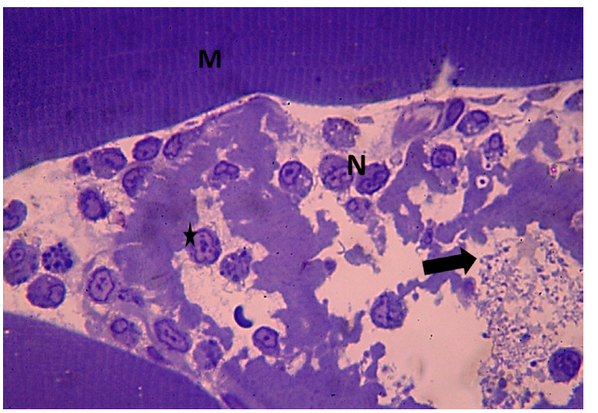

Fig. 21: A photomicrograph of longitudinal section of rat's gastrocnemius of subgroup IIIA showing necrotic debris (arrow), neutrophil (N) and macrophage (star). Notice nearby normal myofibers with prominent striations (M). Toluidine blue (X1000)

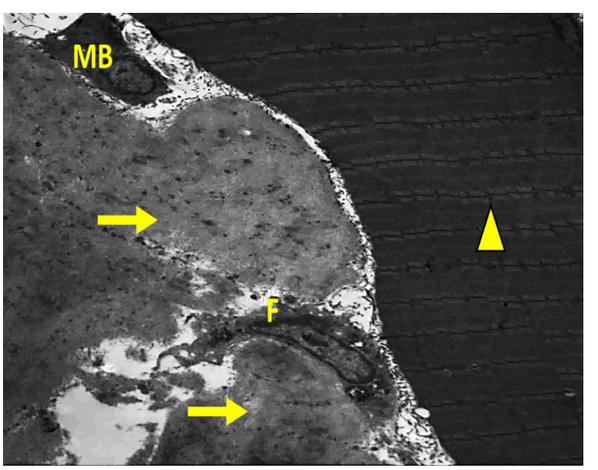

Fig. 22: A photomicrograph of longitudinal section of rat's gastrocnemius of subgroup IIIA showing necrotic myofibers (arrow) with complete loss of muscle striation separated from nearby normal architecture muscle fibers (arrowhead). Notice, mononuclear myoblast cell (MB). Note also spindle shaped fibroblast(F). TEM (X1200)

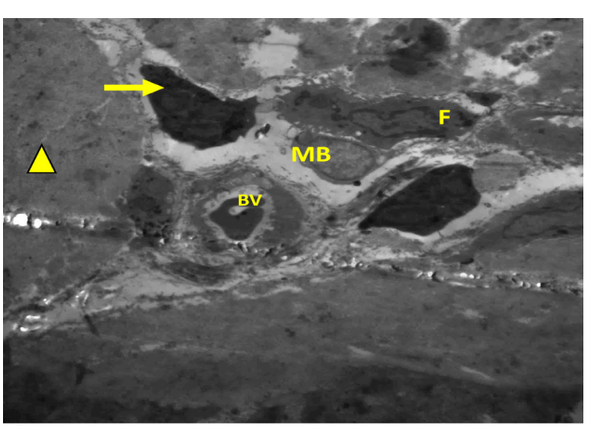

Fig. 23: A photomicrograph of longitudinal section of rat's gastrocnemius of subgroup IIIA showing necrotic myofibers with complete loss of muscle striation (arrowhead). Notice myoblast cell (MB), multilobed nucleus neutrophil (arrow), spindle shaped fibroblast (F) and blood vessel (BV). TEM (X1000)

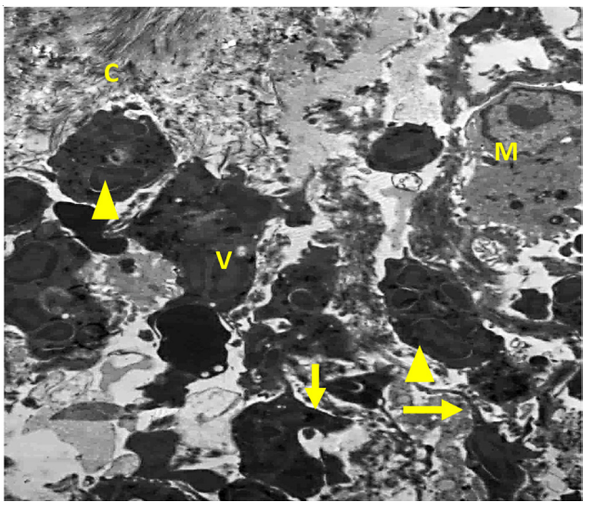

Fig. 24: A photomicrograph of longitudinal section of rat's gastrocnemius of subgroup IIIA showing numerous neutrophils (arrowhead). Some of them showing membrane bound cytoplasmic extensions as pseudopodia around necrotic debris (arrow), while others showing vesicles (V). Notice macrophages (M) and collagen fibers deposition (C). TEM (X1000)

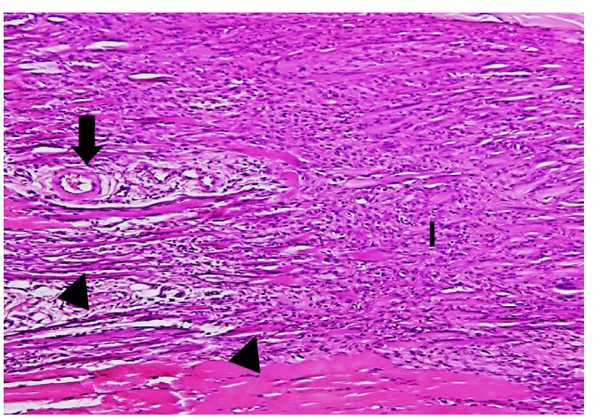

Fig. 25: A photomicrograph of longitudinal section of rat's gastrocnemius of subgroup IIIB showing many regenerated muscle fibers (arrowhead) surrounded by inflammatory cell infiltrate (I). Notice newly formed blood vessels (arrow). H&E (X100)

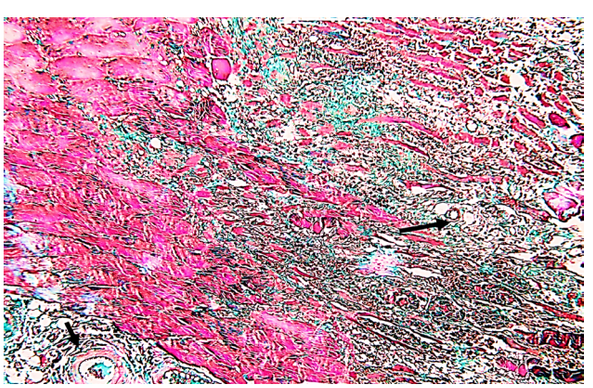

Fig. 26: A photomicrograph of longitudinal section of rat's gastrocnemius of subgroup IIIB showing tightly packed, green-colored bundles of collagen fibers deposition among newly formed red colored myofibers. Notice blood vessels (arrow). Masson's trichrome (X100)

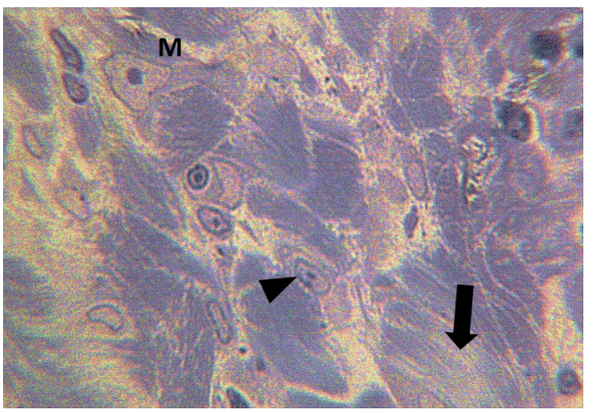

Fig. 27: A photomicrograph of longitudinal section of rat's gastrocnemius of subgroup IIIB showing numerous myofilament (arrow) and mononuclear myoblast cell (arrowhead). Notice macrophage (M). Toluidine blue (X1000)

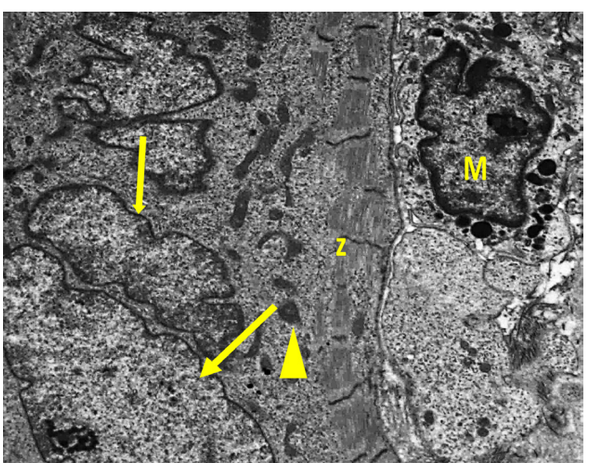

Fig. 28: A photomicrograph of ultrathin section of rat's gastrocnemius of subgroup IIIB showing well-formed multinucleated (arrow) myotube with numerous mitochondria (arrowhead) and myofilaments that show z line, macrophages (M) are seen in contact with myotube. TEM (X2000)

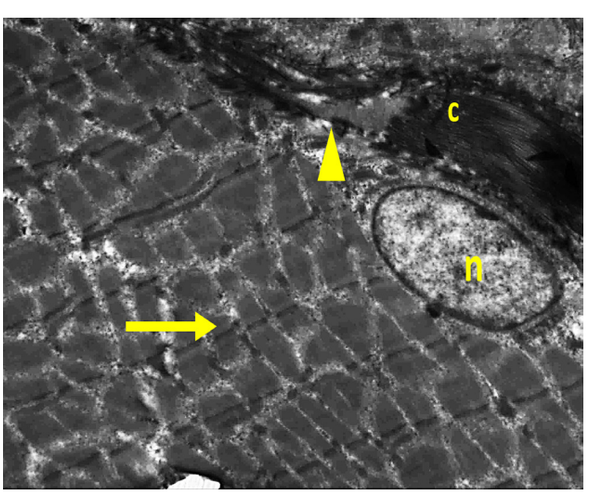

Fig. 29: A photomicrograph of ultrathin section of gastrocnemius of subgroup IIIB rats showing nearly organized sarcomeres with peripheral nucleus (n) and intact sarcolemma (arrowhead). Collagen fibers deposition is seen in between myofibers (C). TEM (X2000)

Table 1: Showing mean number of inflammatory cells.

	Subgroup IIA	Group II (Untreated Muscle Injury Group)		Group III (PRP Treated Muscle Injury Group)	
		Subgroup IIB	Subgroup IIIA	Subgroup IIIB	
	Mean ± SD of inflammatory cells	15.4 ±1.14	38.76 ±4.38	96.76 ±1.92	27.8 ±2.49
T test	Between Subgroup IIA & IIIA	($P < 0.001^{**}$)			
T test	Between Subgroup IIB & IIIB	($P < 0.001^{**}$)			

(**= Highly Significant)

Table 2: Showing mean number of regenerating myofibers.

	Subgroup IIB	Group II (Untreated Muscle Injury Group)	Group III (PRP Treated Muscle Injury Group)
		Subgroup IIIB	
	Mean ± SD of regenerating myofibers	5.2 ±2.39	17.8 ±1.92
T test	Between Group IIB &IIIB	($P < 0.001^{**}$)	

(**= Highly Significant)

Table 3: Showing mean of collagen fibers deposition.

	Subgroup IIA	Group II (Untreated Muscle Injury Group)		Group III (PRP Treated Muscle Injury Group)	
		Subgroup IIB	Subgroup IIIA	Subgroup IIIB	
	Mean ± SD of collagen fibers deposition	14.51 ±1.62	43.19 ±7.87	14.21 ±1.56	26.37 ±3.55
T test	Between Subgroup IIA & IIIA	($P > 0.05^{Ø}$)			
T test	Between Subgroup IIB & IIIB	($P < 0.05^{*}$)			

(* = Significant and Ø = non-significant)

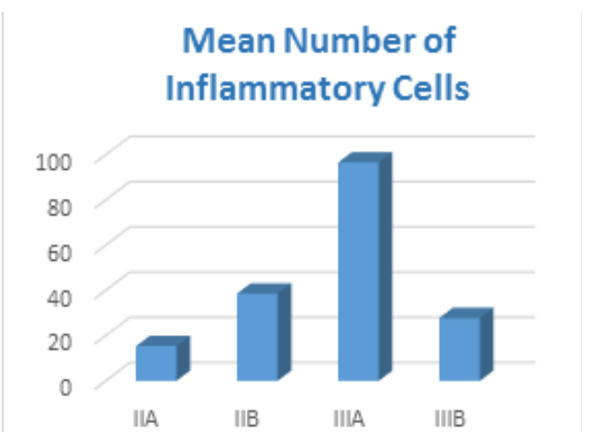

Histogram 1: demonstrating the morphometric comparison between the subgroups IIA, IIB, IIIA & IIIB as regards mean number of inflammatory cells

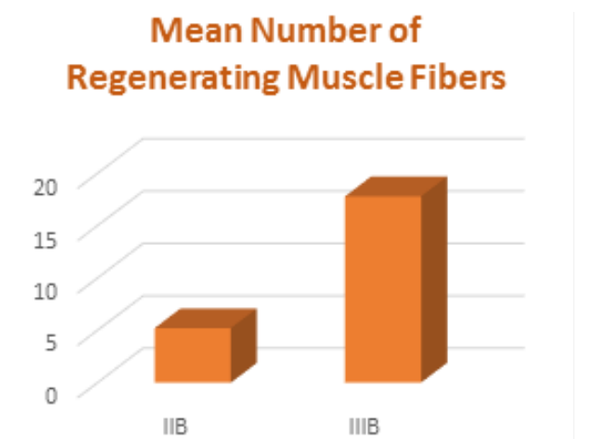

Histogram 2: demonstrating the morphometric comparison between the subgroups IIB & IIIB as regards mean number of regenerating myofibers

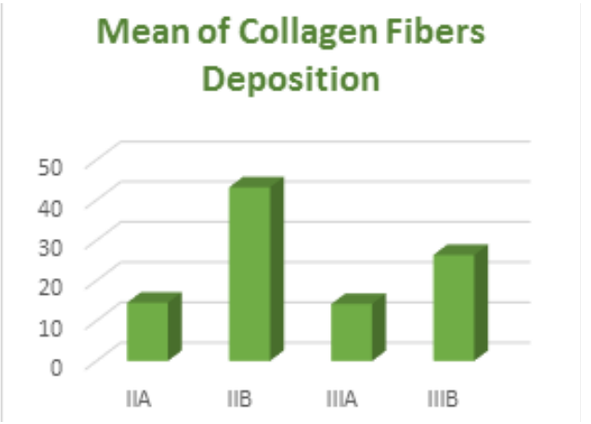

Histogram 3: demonstrating the morphometric comparison between the subgroups IIA, IIB, IIIA & IIIB as regards mean area percentage of collagen fibers deposition

DISCUSSION

Muscle injury is one of the most frequently encountered injuries that occur by various degrees especially in elderly people and usually ends up with incomplete functional recovery in this age group due to fibrosis[14,15].

In the present study, muscle injury in both the untreated and PRP treated rats sacrificed one day after injury (subgroups IIA and IIIA respectively) revealed many common degenerative signs including; markedly damaged myofibers, focal areas of hemorrhage and widening of the interstitial space with edema. Similarly, it has been reported that the first day after muscle injury was considered to be a degenerative phase characterized by disruption of muscle ultrastructure with necrosis of the damaged myofibers with subsequent chemotactic recruitment of inflammatory cells and hematoma formation[16,17]. Moreover, vascular permeability and hydrostatic pressure have been found to increase within the vessels after injury in order to overcome the osmotic pressure of plasma proteins leading to widening of interstitial spaces thus forcing fluid and plasma exudate out into the interstitial tissue leading to swelling and edema[18] which could explain the mechanism underlying similar findings observed in these two subgroups.

However, the inflammatory response of these two subgroups (IIA & IIIA) showed obvious differences. It has been reported that aging was accompanied by persistent muscular inflammation in resting muscles and on the other hand, in case of acute damage the inflammatory response showed obvious reduction[19]. Moreover, the number of T cells got lower with age thus affecting muscle regeneration[20]. However, the present study clarified this fact and reinforced the beneficial effects of PRP in senile rats by the highly significant increase in the number of inflammatory cells in the PRP treated subgroup IIIA when compared to untreated subgroup IIA (P <0.001). This finding revealed stronger post injury inflammatory response in senile rats of the PRP treated group. Similarly, it has been previously observed that the infiltration of leukocytes in muscles injected with PRP was significantly higher than that in the untreated muscles[21]. Moreover, PRP has been found to promote tissue repair by increasing the number of leukocytes at the damaged site[22]. This has been explained by Andia and Abate[23], who reported that active platelets in PRP produced many chemokines through their alpha granules which worked with innate immune cells like neutrophils and monocytes to create a proinflammatory environment.

On the other hand, injured muscles of rats that were left to be sacrificed on the 7th day after injury revealed marked differences between the untreated and the PRP treated subgroups (IIB & IIIB respectively). Muscles of untreated rats showed weak reparative signs where the regenerated myofibers were few, widely separated with irregularly organized sarcomeres and sarcoplasmic vacuolation. Moreover, numerous nearby necrotic debris, macrophages and mononuclear myoblast cells were also detected. On the other hand, PRP treated rats revealed obvious reparative signs where numerous regenerated muscle fibers were massively seen. These regenerated myofibers were well formed with numerous mitochondria and myofilaments with obvious Z lines. In addition, macrophages were frequently seen connected to newly formed myofibers. This cell-to-cell contact and interaction between myoblasts and macrophages has been reported at every stage throughout normal myogenesis, beginning with the recruitment of activated satellite cells (SCs) and progressing through the growth of myotubes[24]. Macrophages affect muscle repair by secreting cytokines such as Interferon-γ, TNF-α, and IL-6 which control immune cells, and SCs activities[25]. Aging was found to be accompanied by notable decrease in the number as well as the function of SCs[26]. It has been found that PRP could induce SC activation with subsequent proliferation, migration, and differentiation into myoblast forming multinucleated myotubes and, eventually, myofibers. Moreover, it expands the diameter of regenerating myofibers thus speeding up the process of muscle regeneration[27,28]. In addition, many of these myoblasts could fuse with the existing injured myofibers during necrosis, preventing further muscle fiber degeneration[28]. Moreover, statistical results of the present study further clarified the PRP reparative role where the number of regenerating myofibers in the PRP treated subgroup (IIIB) showed highly significantly increase in comparison to the untreated subgroup (IIB) ($P < 0.001$).

Regarding the inflammatory response in the same two subgroups, untreated subgroup IIB showed significant increase in the mean number of inflammatory cells when compared to the PRP treated subgroup IIIB ($P < 0.05$). This finding indicates delayed inflammatory response in the untreated rats which significantly subsided in the PRP treated ones. It has been previously stated that aging had an impact on the immune system, giving rise to inflammaging, in which immune cells have a stronger pro-inflammatory characteristic and fail to entirely resolve the inflammation that is why skeletal muscle healing is slower in older mice[29]. Moreover, the function of neutrophils gradually

becomes dysregulated during the aging process and plays a key part in the low-level chronic inflammatory process with subsequent local tissue damage[30]. On the other hand, it has been found that PRP injection reduced the inflammatory marker CD68-positive cells at day 2 following injury and improved muscle recovery by reducing inflammation and apoptosis[27]. PRP could also regulate the function of TNF-α, IL-1β, IL-6 and speed up the inflammatory phase, attracting leukocytes, macrophages, and fibroblasts to the injury site to clear debris thus initiating healing progression and speeding up recovery[31]. Thus, PRP prevents the persistence of post injury delayed inflammatory response.

As for the amount of collagen fibers formed by the 7th day post injury, Masson's trichrome stained sections of the present study revealed marked deposition of densely packed, greenish-colored collagen fibers bundles in the damaged site with some intervening regenerating myofibers in the untreated subgroup IIB while the PRP treated subgroup IIIB showed some tightly packed collagen fibers among numerous newly formed myofibers and numerous blood vessels. Age related healing by fibrotic scar has been attributed to the associated unregulated inflammatory response causing oxidative stress with excessive release of extra TGF-β in the damaged muscle of old rats which promotes collagen I expression and formation of fibrotic connective tissue[32]. On the other hand, PRP application has been found by some studies to reduce fibrous scars from injured skeletal muscles whether used alone or in combination with antifibrosis medicines[33]. Moreover, its application in injured muscles has been reported to decrease the fibrous tissue area and to shift it away from fibrosis toward the complete muscular regeneration in chronic hyperglycemic rats[34]. This could be attributed to anti-fibrotic substances such as hepatocyte growth factor (HGF) and serum amyloid protein in the PRP, which could suppress fibrosis and control macrophage activity[35]. This could explain the antifibrotic effects of PRP noted in the present study which was further reinforced by statistical results that revealed highly significant decrease in the mean area percentage of collagen fibers deposition in the PRP treated subgroup IIIB compared to the untreated IIB.

Among the previous studies that examined the reparative effects of PRP on injured muscles of adult rats, Quarteiro *et al*.,[11] reported that PRP significantly enhanced the inflammatory response by the 7th day post injury with marked decrease in collagen fibers' deposition.

The present study further reinforced these beneficial reparative effects of PRP on injured muscles of senile rats by the 7th day compared to the ones left without treatment. Platelet rich plasma led to stronger post injury acute inflammatory response and prevented the persistence of the previously recorded age-related delayed inflammatory state. Moreover, it markedly enhanced myogenesis and decreased fibrous tissue scaring.

Conclusion

Platelet rich plasma treatment accelerated the rate and improved the quality of skeletal muscle healing from injury in senile rats.

RECOMMENDATION

Further studies with longer duration for the effects of PRP on injured muscles of senile rats are recommended.

CONFLICT OF INTERESTS

There are no conflicts of interest.

REFERNCES

1. Contreras-Munoz p, Torrella JR, Serres X, Rizo-Roca D, Varga M, Viscor G, *et al*. post-injury exercise and platelet-rich plasma therapies improve skeletal muscle healing in rats but are not synergistic when combined. Am J Sports Med 2017; 45(9):2131-2141.doi: 10.1177/0363546517702864.
2. Chen W, Lin H, Lee C, and Chen Y. Aged skeletal muscle retains the ability to remodel extracellular matrix for degradation of collagen deposition after muscle injury. Int J Mol Sci 2021; 22(4):2123.doi: 10.3390/ijms22042123.
3. Rubenstein LZ. Falls in older people: epidemiology, risk factors and strategies for prevention. Age Ageing 2006;35(2): ii37-ii41.doi: 10.1093/ageing/afl084.
4. Martins L, Gallo CC, Honda TS, Alves PT, Stilhano RS, Rosa DS, *et al*. Skeletal muscle healing by M1-like macrophages produced by transient expression of exogenous GM-CSF. Stem Cell Res Ther 2020 ; 11(1): 473.doi: 10.1186/s13287-020-01992-1.
5. Everts P, Onishi K, Jayaram P, Lana JF, and Mautner K. Platelet-rich plasma: new performance understandings and therapeutic considerations in 2020. Int J Mol Sci 2020; 21(20):7794.doi: 10.3390/ijms21207794.
6. Sharma A, Fish B, Moulder J, and Cohen EP.: Safety and blood sample volume and quality of a refined retro-orbital bleeding technique in rats using a lateral approach. Lab Anim 2014; 43(2): 63–66.doi: 10.1038/laban.432.
7. Garciaa TA, Ozakia GA, Castoldia RC, Koikeb TE, Camargoc RC, and Filho JC. Fractal dimension in the evaluation of different treatments of muscular injury in rats. Tissue Cell 2018; 54:120–126. doi: 10.1016/j.tice.2018.08.014.
8. Hammond JW, Hinton RY, Curl LA, Muriel JM, and Lovering RM. Use of Autologous Platelet-rich Plasma to Treat Muscle Strain Injuries. Am J Sports Med 2009;37(6): 1135-1142.doi: 10.1177/0363546508330974.
9. Kunduracioglu B, Ulkar B, Sabuncuoglu BT, Can B, and Bayrakci K. Effects of hypertonic dextrose on injured rat skeletal muscles. J Neurosci 2006; 11(2): 93-96.PMID: 22266556.
10. Russ DW, Garveyc SM, Densmorea C, Hawksa T, Hermana S, and Pardia K. Effect of acute muscle contusion injury, with and without dietary fish oil, on adult and aged male rats: contractile and biochemical responses. Exp Gerontol 2018;111: 241–252.doi: 10.1016/j.exger.2018.08.001.
11. Quarteiro ML, Tognini JRF., Flores de Oliveira EL, and Silveira I. The Effect of Platelet-Rich Plasma on The Repair of Muscle Injuries in Rats. REV BRAS ORTOP 2015; 50(5):586–595.doi: 10.1016/j.rboe.2015.08.009.
12. Gamble M and Bancroft JD. Theory and practice of histological techniques.6th ed. London. Churchill Livingstone. 2008; 121–135.
13. Suvarna SK, Layton C and Bancroft JD. Bancroft's theory and practice of histological techniques. 7th ed. Churchill Livingstone. ElSevier. 2013; 224, 408-411.

14. Qazi TH, Duda GN, Ort MJ, Perka C, Geissler S and Winkler T. Cell therapy to improve regeneration of skeletal muscle injuries. J Cachexia Sarcopenia Muscle 2019; 10: 501–516.doi: 10.1002/jcsm.12416

15. Distefano G and Goodpaster BH. Effects of Exercise and Aging on Skeletal Muscle. Cold Spring Harb Perspect Med 2018; 8(3):a029785.doi: 10.1101/cshperspect.a029785.

16. Jarvinen TA, Jarvinen TL, Kaariainen M, Kalimo H, and Jarvinen M. Muscle injuries: biology and treatment. Am J Sports Med 2005;33(5):745-764.doi: 10.1177/0363546505274714.

17. Garg K, Corona BT, and Walters TJ. Therapeutic strategies for preventing skeletal muscle fibrosis after injury. Front Pharmacol 2015; (6):87.doi: 10.3389/fphar.2015.00087.

18. Rutkowski MJ, Sughrue ME, Kane AJ, Ahn BJ, Fang S, and Parsa AT. The complement cascade as a mediator of tissue growth and regeneration. Inflamm Res 2010; 59(11): 897-905.doi: 10.1007/s00011-010-0220-6.

19. Tobin SW, Alibhai F, Wlodarek L, Yeganeh A, Millar S, Wu J, *et al*. Delineating the relationship between immune system aging and myogenesis in muscle repair. Aging Cell 2021;20(2)e13312. doi: 10.1111/acel.13312.

20. Schiaffino S, Pereira MG, Ciciliot S, and Rovere-Querini P. Regulatory T cells and skeletal muscle regeneration. FEBS J 2017; 284(4) 517–524.doi: 10.1111/febs.13827.

21. Borrione P, Grasso L, Chierto E, Geuna S, Racca S, Abbadessa G, *et al*. Experimental model for the study of the effects of platelet-rich plasma on the early phases of muscle healing. Blood Transfus 2014;12(1):221-228.doi: 10.2450/2013.0275-12

22. Li H, Usas A, Poddar M, Chen C, Thompson S, Ahani B, *et al*. Platelet-Rich plasma promotes the proliferation of human muscle derived progenitor cells and maintains their stemness. PLoS One 2013;8(6): e64923.doi: 10.1371/journal.pone.0064923

23. Andia I, and Abate M. Platelet-rich plasma: underlying biology and clinical correlates. Regenerative medicine 2013;8(5):645-58.doi: 10.2217/rme.13.59.

24. Ceafalan LC, Fertig TE, Popescu AC, Popescu BO, Hinescu ME, and Gherghiceanu M. Skeletal muscle regeneration involves macrophage-myoblast bonding. Cell Adh Migr 2018;12(3):228-35. doi: 10.1080/19336918.2017.

25. Oishi Y., and Manabe I. Macrophages in inflammation, repair, and regeneration. Int Immunol 2018; 30(11):511-28.doi: 10.1093/intimm/dxy054.

26. Garcia-Prat L, Sousa-Victor P, and Munoz-Canoves P. Functional dysregulation of stem cells during aging: A focus on skeletal muscle stem cells. FEBS J 2013; 280:4051-4062.doi: 10.1111/febs.12221.

27. Tsai WC, Yu TY, Chang GJ, Lin LP, Lin MS, and Pang JS. Platelet-rich plasma releasate promotes regeneration and decreases inflammation and apoptosis of injured skeletal muscle. Am J Sports Med 2018;46(8):1980-1986.doi: 10.1177/0363546518771076.

28. Oberlohr V, Lengel H, Hambright W, Whitney K, Evans T, and Huard J. Biologics for skeletal muscle healing: the role of senescence and platelet-based treatment modalities. Oper Tech Sports Med 2020;28(3):150754.doi:10.1016/j.otsm.2020.150754

29. Panci G. and Chazaud B. Inflammation during post-injury skeletal muscle regeneration. Semin Cell Dev Biol 2021; 119:32–38.doi: 10.1016/j.semcdb.2021.05.031.

30. Butcher S, Chahel H, and Lord JM. Review article: ageing and the neutrophil: no appetite for killing. Immunology 2000;100(4): 411–416.doi: 10.1046/j.1365-2567.2000.00079.x

31. Borrione P, Fagnani F, Di Gianfrancesco A, Mancini A, Pigozzi F, and Pitsiladis Y. The role of platelet-rich plasma in muscle healing. Curr Sports Med Rep2017;16(6):459-463.doi: 10.1249/JSR.0000000000000432.

32. Ghaly A, and Marsh DR. Aging-associated oxidative stress modulates the acute inflammatory response in skeletal muscle after contusion injury. Exp Gerontol 2010;(45) 381–388.doi: 10.1016/j.exger.2010.03.004.

33. Li H, Hicks JJ, Wang L, Oyster N, Philippon M, Hurwitz S, *et al*. Customized platelet-rich plasma with transforming growth factor b1 neutralization antibody to reduce fibrosis in skeletal muscle. Biomaterials 2016; 87:147-156.doi: 10.1016/j.biomaterials.2016.02.017.

34. Rtail R, Maksymova O, Illiashenko V, Gortynska O, Korenkov O, Moskalenko P, *et al*. Improvement of skeletal muscle regeneration by platelet-rich plasma in rats with experimental chronic hyperglycemia. BioMed Res Int 2020; 6980607.doi: 10.1155/2020/6980607

35. Sugiura T, Kawaguchi Y, Soejima M, Katsumata Y, Gono T, Baba S, *et al*. Increased HGF and c-Met in muscle tissues of polymyositis and dermatomyositis patients: beneficial roles of HGF in muscle regeneration. Clin Immunol 2010; 136(3):387-99.doi: 10.1016/j.clim.2010.04.015.

الملخص العربى

تأثير البلازما الغنية بالصفائح الدموية مقابل التجدد التلقائي في الإصابة المستحثة للعضلات في ذكور الجرذان البيضاء المسنة

يارا حسن محمد[١]، شهيرة يوسف ميخائيل[٢]، رحاب طلبه خطاب[٢]، نهى محمد جابر[٢]، هالة طه شعلان[٢]، ماري رفعت اسحق[٢]

قسم التشريح وعلم الاجنة، كلية الطب، [١]جامعة السويس، [٢]جامعة عين شمس، مصر

المقدمة: يعتبر السقوط مع ما يصاحبه من كسور وإصابة للعضلات شائع جدا في كبار السن. وقد وجد أن البلازما الغنية بالصفائح الدموية لديها قدرة ملحوظة على تعزيز تجديد الأنسجة والأعضاء المختلفة كما يتم تطبيقها في الوقت الحالي على نطاق واسع في مجموعة متنوعة من القطاعات الطبية.

الهدف من البحث: هدفت الدراسة الحالية الى معرفة تاثير البلازما الغنية بالصفائح الدموية على إلتئام العضلات الهيكلية في ذكور الجرذان البيضاء المسنة.

المواد وطرق البحث: تم استخدام اثنتان و أربعون من ذكورالجرذان البيضاء المسنة, البالغة من العمر ٢٤ شهرا و يبلغ وزنها حوالي ٢٨٠ جرام, في هذه الدراسة. ستة جرذان تم تعيينهم كمتبرعين بالبلازما الغنية بالصفائح الدموية و تم تقسيم الستة والثلاثون الآخرون بالتساوي إلى ثلاث مجموعات :

المجموعة الاولى: قسمت بالتساوى الى مجموعتين فرعيتين؛

- المجموعة الفرعية الاولى أ: و قد تركت دون أي تدخل .
- المجموعة الفرعية الاولى ب: تم إجراء عملية تتمثل في احداث جرح بالجلد فقط في الطرف الخلفي الأيمن للجرذان مع الحفاظ على عضلة بطن الساق سليمة.

المجموعة الثانية: تم احداث إصابة بعضلة بطن الساق في الطرف الخلفي الايمن وتركت الجرذان للإستشفاء التلقائي وتم تقسيمها بالتساوي الى مجموعتين فرعيتين؛

- المجموعة الفرعية الثانية أ: تم التضحية بهم في اليوم الاول بعد الاصابة.
- المجموعة الفرعية الثانية ب: تم التضحية بهم في اليوم السابع بعد الاصابة.
- المجموعة الثالثة: تم احداث إصابة بعضلة بطن الساق مع علاج الجرذان باستخدام ١٠٠ ملل من البلازما الغنية بالصفائح الدموية في يوم الإصابة ثم قسمت الجرذان بعد ذلك بالتساوي الى مجموعتين فرعيتين:
- المجموعة الفرعية الثالثة أ: تم التضحية بهم في اليوم الاول بعد الإصابة.
- المجموعة الفرعية الثالثة ب: تم إعطائهم١٠٠ ملل من البلازما الغنية بالصفائح الدموية في اليوم الثالث واليوم الخامس ثم تم التضحية بهم في اليوم السابع بعد الإصابة.

في نهاية التجربة تم استئصال عضلة بطن الساق في كل مجموعة فرعية ومعالجتها للفحص المجهري الضوئي والمجهرالاكتروني النافذ كما اجريت دراسة قياسية وتحليل إحصائي.

النتائج: اظهرت المقاطع النسيجية ان إستخدام البلازما الغنية بالصفائح الدموية قد أدى الى إستجابة الخلايا الإلتهابية الحادة بصورة أقوى بعد الإصابة مباشرة مع منع استمرار الحالة الإلتهابية المتأخرة المصاحبة للشيخوخه. بالاضافة الى ذلك فقد ساهم بشكل ملحوظ في إلتئام العضلات و أدي الي تقليل تكوين الأنسجة الليفية.

الخلاصة: أدي استخدام البلازما الغنية بالصفائح الدموية إلى الإسراع في معدل الإلتئام وتحسين في جودة النسيج المتعافي في العضلات الهيكلية المصابة في الجرذان المسنة.